Erosion Prediction in Turbomachinery Resulting from Environmental Solid Particles

G. Grant* and W. Tabakoff†
University of Cincinnati, Cincinnati, Ohio

The erosion resulting from solid particles ingested into rotating machinery is predicted using a Monte Carlo simulation of the physical process. This simulation takes into account the aerodynamic drag on the contaminant particles, the rebound dynamics of the particles impacting the solid blades or channel walls and the material removal process. The computerized model is used to predict the quantity of material removed from the stationary and rotating blades of a turbomachine as well as the location of the erosion on the blades. This model is verified by testing a specially designed one and one-half stage test compressor and measuring the erosion.

Nomenclature

C_D = drag coefficient
IGV = inlet guide vane
M = total mass of particles impacting a target surface
m = mass of an individual particle
Re = Reynolds number
S = distance that a particle travels relative to a particle of fluid
t = time
U = fluid velocity
U^* = characteristic velocity (δ/τ)
V = particle velocity
W = relative velocity ($V-U$)
β = relative angle between particle path and specimen surface
δ = characteristic length (10/3) (D) (ρ_p/ρ_f)
ϵ = erosion per unit mass of impacting particles
μ = dynamic viscosity
ν = kinematic viscosity
ρ = density
σ = standard deviation of a normal distribution
τ = Stokes constant ($\rho_p D^2/18\mu$)

Subscripts

0 = initial state
1 = conditions of the particle approaching the target
2 = conditions of the particle rebounding from the target
f = fluid
p = particle

Introduction

In operating helicopter gas turbine engines in dusty environments, dust clouds are generated which contain particles as large as 200 μ mean diameter. The severity of the damage caused by this dust can be judged from the fact that a 1000 hp engine commonly used for helicopters is considered to have a potential life of only 10 hr when operated continuously in the comparatively moderate dust concentration of about 1 mg/ft^3, i.e., ingestion of approximately 13 lb of sand. Conventional aircraft with low slung inlets have a similar problem. The damage is principally caused by erosion of the compressor blading and is manifested in an axial machine by pitting and cutting back of the leading edges and thinning of the trailing edges.[1] Air filtration and blade coatings have been used for fixes of this problem; however, filtration reduces both payload and performance and blade coatings cannot usually be applied in thickness adequate for developing full effectiveness.

The problem of predicting erosion in the rotating machinery of gas turbines is extremely complex and has not been satisfactorily discussed in the literature. This complexity is primarily a result of the fact that the particle trajectory must be traced through the flowfield after multiple impacts. When a sand particle collides with a high-speed rotor, the erosion can be predicted in a conventional manner if coordinates relative to the rotor are chosen. However, after impacting the rotor and causing the subsequent erosion, the sand particle will rebound with an even higher velocity with respect to the stator and will cause serious damage to it. Further, the particle dynamics resulting from these impacts cause the contaminant particle to centrifuge to the blade tips where the localized high concentration causes severe damage to this very vulnerable region.

The model reported herein solves this problem by using a Monte Carlo simulation. The required input parameters such as particle aerodynamics, particle rebound behavior, and material erosion are developed independently and the complex interaction of these parameters are determined by the model using statistical processes.

Experimental Apparatus

Erosion Research Facility

A wind tunnel was constructed to obtain the basic erosion data and to photograph the particle impacts. A detailed description of this facility, along with design drawings are found in Ref. 2. The main considerations in designing the test equipment were controlling the primary variables of fluid velocity, particle velocity, particle flow rate, and particle sizes in a representative aerodynamic environment. Provisions are designed into the tester to vary the angle of attack between the abrasive particle and the surface of the test specimen.

Figure 1 is a schematic of the apparatus which fulfills these objectives. As depicted in this illustration, the equipment functions as follows(a measured amount of abrasive grit of a given consistency is placed into the particle feeder, A. The particles are fed into a secondary air source and blown up to the particle injector, C, where it mixes with the main air supply, B. The particles are then accelerated by the high velocity air in a constant area duct, D, and impact the specimen in test section, E. The test dust is then separated from the air by a cyclone separator, G, and collected in a container, H. The test air is then further filtered through a commercial 5 μ filter, F.

The test section was constructed with several different inserts to obtain all of the required data. The channel geometry

Presented as Paper 74-16 at the AIAA 12th Aerospace Sciences Meeting. Washington, D.C., January 30-February 1, 1974; submitted March 1, 1974; revision received November 8, 1974. This work was supported under Grant DA-ARO-D-124-G-154, U.S. Army Research Office—Durham.

Index category: Multiphase Flows and Testing.

*Graduate Research Assistant, presently employed as Engineering Specialist at Northrop Corporation, Beverly Hills, Calif.

†Professor, Department of Aerospace Engineering, University of Cincinnati. Associate Fellow AIAA.

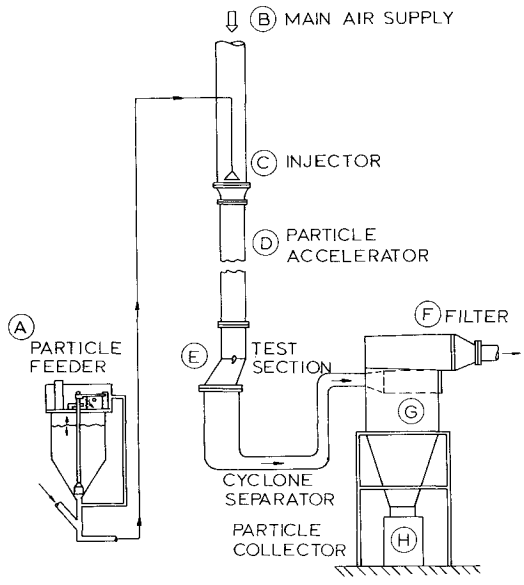

Fig. 1 Erosion test schematic-erosion research facility.

is the same as that of the acceleration section, that is 3 in. × 1 in., up to the location of the specimen where the channel turns 30°. The test section has been designed in such a way as to accommodate a photographic insert through which high speed photography and streak photographs were taken of sand particles. This insert consists of an enclosure plate, a replaceable glass insert and a collar to hold the insert in. The high speed particles scratch the glass through which the pictures are taken, thus this insert is replaced after each test. This unique set facility has resulted in very high quality pictures without disrupting the flowfield.

Rotating Machinery Erosion Facility

This facility was designed to accept a model piece of rotating turbomachinery. The primary purpose of the test in this facility was experimental verification of the analytical model. It functions similar to the facility just described.

Development of Aerodynamic Particle Force Equations

The drag force on small dust particles is usually defined as:

$$F = \tfrac{1}{2}\rho_f w|W|A\,C_D \tag{1}$$

The equation of particle motion is then:

$$m_p\,dV/dt = -\tfrac{1}{2}\rho_f W|W|A\,C_D \tag{2}$$

Thus, in terms of the previous differential equation the particle will be accelerated in the negative direction of the relative velocity vector with a magnitude proportional to the square of the relative velocity.

The drag coefficient (C_D) for spheres, disks, cylinders, and miscellaneous geometric shapes has been obtained experimentally and complied by several authors. The general procedure in theoretical studies of particle behavior has been to assume the particles are spherical with a diameter corresponding to that of the projected area in the direction of W. This is primarily due to the relative ease with which the behavior of particles of other shapes can be deduced from the results on spherical particles. Over the range of Reynolds numbers generally countered the drag coefficient is approximated by the following equation:

$$C_D = 0.4 + 24/Re \tag{3}$$

By assuming that the particles are spherical, the following relations can be written:

$$m_p = \rho_p(\pi/6)D^3;\quad A = (\pi/4)D^2;\quad Re = |W|D\rho_F/\mu \tag{4}$$

Substituting the aforementioned into Eq. (2) and simplifying yields:

$$dV/dt = -W(1/\delta|W| + 1/\tau) \tag{5}$$

where

$$\delta = (10/3)D(\rho_p/\rho_f) \text{ and } \tau = (\rho_p D^2/18\mu)$$

thus the characteristics velocity is:

$$U^* = (\delta/\tau) = 60(\nu/D) \tag{6}$$

and

$$Re = 60(W/U^*) \tag{7}$$

Note that δ has the units of length, and the constant is equivalent to a characteristic length. Further, τ has the units of time and is closely associated with the Stokesian time constant used in calculating the free fall velocity of a sphere. Finally then, U^* has the units of fps and is characteristic velocity associated with this problem.

Equation (5) can be rewritten in terms of the fluid velocity by making the following transformation:

$$W = V\text{-}U$$

which can be differentiated to give:

$$dW/dt = dV/dt - dU/dt \tag{8}$$

Substituting this relationship into Eq. (5) results in the following equation:

$$dW/dt = -W(1/\delta|W| + 1/\tau) - dU/dt \tag{9}$$

The term dU/dt is the acceleration of the fluid as seen by the particle. It does not imply that the flow is unsteady in the conventional sense.

Method of Solution

Equation (9) is a general expression of particle dynamics immersed in a fluid of a different velocity. The solution of this equation is developed by the authors in Ref. 3. Basically the approach is to first solve the fluids problem and store this information on a grid, then integrate the equation using a step-by-step procedure.

The resulting solution will depend on the nature of the coefficients as follows:

Case I: $1 > (4\tau/U^*)(dU/dt)$

$$W/U^* = 0.5\left[(D1 - D2) + B(D1 + D2)/(D2 - D1)\right] \tag{10a}$$

where

$$D1 = [2W_o/U^* + (1 - B)]$$

$$D2 = [2W_o/U^* + (1 + B)]e^B(t - t_o/\tau)$$

$$B = [1 - (4\tau/U^*)(dU/dt)]^{1/2}$$

Case II: $1 < (4\tau/U^*)(dU/dt)$

$$W/U^* = \tfrac{1}{2}[(D1\,B - 1) - (B + D1)D2/1 + (D1)(D2)] \tag{10b}$$

where

$$D1 = (2W_o/U^* + 1)/B \text{ and } D2 = \text{Tan}\,[B/2(t - t_0/\tau)]$$

$$B = [(4\tau/U^*)(dU/dt) - 1]^{1/2}$$

Case III: $1 = (4\tau/U^*)(dU/dt)$

$$(W/U^*) = (W_0/U^*) - \tfrac{1}{2}(D1/1 + D1)$$

where $D1 = (W_0/U^* + \tfrac{1}{2})(t - t_0/\tau)$ (10c)

The relative distance S is solved for as:

$$(S-S_0)/\delta = \tfrac{1}{2}\{\ln[\,[\,(W_0/U^*)^2 + W_0/U^* + \tau/U^*\, dU/dt\,]\,/\,([\,W/U^*)^2 + W/U^* + \tau/U^*\, dU/dt\,]\,] - (t-t_0/\tau)\} \quad (11)$$

Finally, the distance $(x-x_o)$ traveled during time $(t-t_o)$ is solved as follows:

$$\frac{x-x_0}{\delta} = \frac{(U+U_o)}{2U^*}\left[\frac{(t-t_o)}{\tau}\right] + \frac{(S-S_0)}{\delta} \quad (12)$$

Equations (10-12) are used to describe the particle trajectories in the predetermined flowfield using an inertial reference frame. The mechanics of the solution require that the particle be located on the grid system prescribed for the apparatus under investigation. In this manner the parameters δ, τ, U^*, W_o, and dU/dt are determined. From Eq. (2) it can be observed that the vector dV/dt is in the direction of W. In the three-dimensional case dU/dt need not be in the direction of W. In this case dU/dt os expressed as component parallel to and perpendicular to W and Eq. (9) becomes the parallel component to W,

$$\frac{dW}{dt} = -W\left(\frac{|W|}{\delta} + \frac{1}{\tau}\right) - \frac{dU}{dt}$$

and the perpendicular component to W,

$$dW/dt = -dU/dt$$

After solving these vector equations, in an inertial reference frame, the particle is relocated on the grid by means of direction cosines. In practice an iteration scheme is used to obtain the average values of the parameters over the interval under consideration. This method of solution has the advantage that the particle dynamic equations are independent of the coordinate system used to store the fluid dynamic information within the machine. The method of solution is detailed in Ref. 3.

Development of Particle Rebound Correlations

The erosion of metals impacted by small dust particles as well as the rebound dynamics of these particles can only be described in a statistical sense. This becomes obvious when one examines the number of geometric situations that might occur at impact. After a given incubation period, the target material will become pitted with craters and in fact after a slightly longer period, a regular ripple pattern may form on the eroded surface.[4] Thus, the local impact angle between the small particle and the eroded surface may deviate considerably from the geometric average. Further, the particles themselves are irregular crystalline in shape with several sharp corners. As the particle approaches the specimen the orientation of the particle is, for the most part, random. Thus, some particles will impact on a flat surface and do very little work on the target material. Others will impact with a corner oriented in a manner where it will remove material in a method similar to that of a cutting tool. This effect of particle orientation on erosion has been discussed in the literature.[5,6]

The statistical study required a somewhat lengthly analysis due to the large number of impacts that were examined. This fact limited the number of cases that were tested. The final test program consisted of four tests which examined the effect of angle of attack as well as particle velocity. Variables that could be of importance but not analyzed were particle material, target material, and particle size. Quartz sand was picked due to its high reflective properties. Alumina sand was tried but the photographic results were not of sufficient quality to be used. The target material used was annealed 2024 aluminum alloy and the particle size was 200μ. The experimental variables examined are described in Table 1.

Table 1 Summary of Results[a]

Restitution ratio parameter	Incoming angle of attack	Incoming particle velocity	Sample statistical mean	Standard deviation	Sample size (#)
Velocity	20°	250 fps	0.697	0.1503	207
	45°	250	0.550	0.1445	121
V_2/V_1	45°	390	0.400	0.1469	177
	90°	250	0.210	0.0655	253
	20°	250	0.525	0.2941	207
V_{n_2}/V_{n_1}	45°	250	0.362	0.1367	121
	45°	390	0.334	0.1391	177
	90°	250	0.176	0.0616	253
	20°	250	0.600	0.1529	207
V_{t_2}/V_{t_1}	45°	250	0.717	0.2019	121
	45°	390	0.654	0.2220	177
	90°	250	...	...	253
	20°	250	0.921		207
	45°	250	0.626		121
β_2/β_1	45°	390	0.633		177
	90°	250	0.683		253

[a] Target Material, 2024 aluminum alloy; particle material, silica sand (quartz); particle size, 200μ.

Before the particle impacted the specimen, it was accelerated a distance of slightly over 12 ft such that the particle velocity was very close to the air velocity. High speed movies were taken to record the impact phenomenon. This method of recording the data was chosen as it allowed a large number of data points to be photographed at almost the same time, thus keeping the conditions of flow constant and enabling an accurate assessment of the particle environment to be made. The photographic methods and techniques to obtain data are described by the authors in Ref. 7.

On Figs 2 and 3 the ratio of the particle velocity components normal and tangential to the surface of the specimen are plotted against the angle of attack (β_1). Since the statistical distributions are important, the shape of these distributions are cross plotted on these figures. Further, the data obtained by Hussein[8] for nonerosive particles (corncobs) are plotted on this figure for comparison. The restitution ratio parameter (V_2/V_1) is a measure of the momentum lost by the particle at impact and as such should correlate with the work done on the target material and thus erosion. In Fig. 2 the normal component of the restitution ratio ($V_{N2}/V_{N1} = V_2 \sin\beta_2/V_1 \sin\beta_1$) is plotted against the angle of attack (β_1). The spread in the statistical data at low angles is most likely due to the irregularity of the surface. In Fig. 3, the tangential or parallel component of the restitution ratio ($V_{T_2}/V_{T_1} = V_2 \cos\beta_2/V_1 \cos\beta_1$) is plotted. The statistical distributions of these data appear to be reasonably tight and well formed. The average value of V_{T_2}/V_{T_1} is the only parameter analyzed which support the theory that erosion is proportional to a particle momentum loss at impact. The maximum erosion of the material tested (2024 aluminum) occurs at β_1 of 20°. This is also where the V_{T_2}/V_{T_1} reaches a minimum.

These results indicate that the normal component of velocity does not significantly contribute to ductile erosion. Most probably the kinetic energy is dissipated by plastic deformation of the target material without significant material removal. On the other hand, the loss of the tangential component of the particle velocity at impact does correlate with the erosion results. These facts support the model of erosion proposed by Finnie.[5]

The solid lines in Figs. 2 and 3 represent a least squares polynominal curve fit of the mean value of the restitution parameter and may be expressed by the equations:

$$V_{N_2}/V_{N_1} = 0.993 - 1.76\beta_1 - 1.56\beta_1^2 - 0.49\beta_1^3 \quad (13)$$

$$V_{T_2}/V_{T_1} = 0.988 - 1.66\beta_1 + 2.11\beta_1^2 - 0.67\beta_1^3 \quad (14)$$

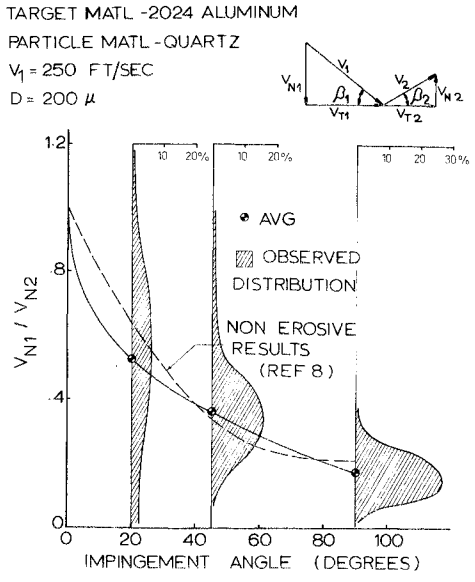

Fig. 2 Influence of impact angle on the erosive particle normal velocity restitution ratio.

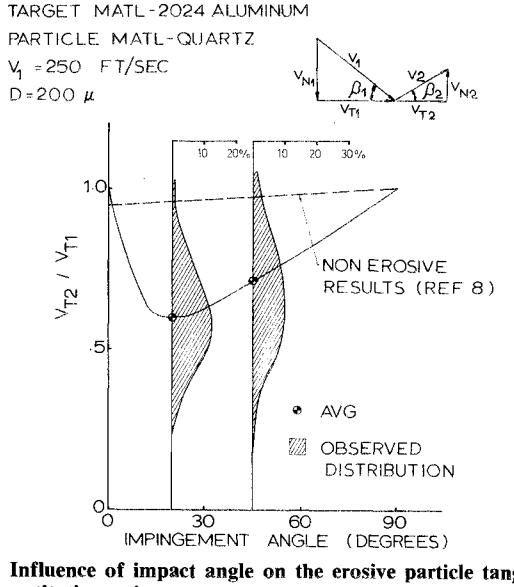

Fig. 3 Influence of impact angle on the erosive particle tangential velocity restitution ratio.

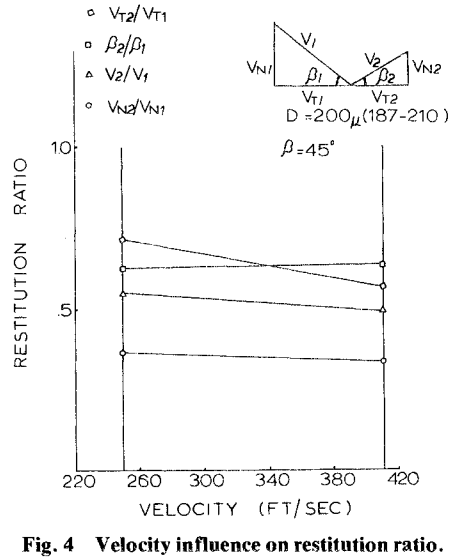

Fig. 4 Velocity influence on restitution ratio.

Equations for the standard deviation of the normal and tangential velocity restitution ratio were also obtained so that the effect of impact angle on the statistical behavior of these parameters could be duplicated in the prediction model. These equations are as follows:

$$\sigma(V_{T_2}/V_{T_1}) = -0.0005 + 0.62\,\beta_1 - 0.535\,\beta_1^2 + 0.089\,\beta_1^3 \quad (15)$$

$$\sigma(V_{N_2}/V_{N_1}) = 0 + 2.15\,\beta_1 - 5.02\,\beta_1^2 + 4.05\,\beta_1^3 - 1.085\,\beta_1^4 \quad (16)$$

where $\sigma(N)$ is the standard deviation of the parameter in question.

The average or mean values of the restitution ratio parameters against velocity is plotted in Fig. 4. Since only two different velocities were tested, it was felt that the specific results should not be overly stressed. Further, these levels of velocity are well below conventional rotor tip speeds which is due to a limitation in camera speed. However, the levels of velocity observed are sufficiently high to cause plastic flow which is the basic mechanism of ductile erosion. The validity of the predictive expressions is of course finally measured by the ability of the final model to predict observed results.

Other authors[8-10] have assumed the restitution ratio to be invarient to the magnitude of the approach velocity (after an initial incubation velocity of a few feet per second). However, it can be seen in Fig. 4, or in the data of Table 1, that this is not necessarily so as the tangential restitution ratio appears to be very susceptible to the magnitude of the approach velocity. This fact is especially important since it is this parameter that most influences the erosion rate of the target material.

In summary, the required equations for the restitution ratios have been developed. Further, the nature of the restitution coefficients themselves have been analyzed to provide a basis for an erosion prediction model.

Development of Erosion Equations

The erosion test facility, described previously, was designed in such a manner that the erosion could be measured without destroying the aerodynamics environment. Care was also taken to insure that the surface finishes of the specimen were similar prior to testing. The erosion was determined by measuring the weight of the specimen before and after testing. The abrasives used were alumina (Al_2O_3) and quartz (SiO_2) obtained from commercial suppliers.

Parameters such as angle of attack, particle velocity, and duration of erosion can strongly influence the extent of the erosion damage and hence received close attention in this study. Other parameters such as particle concentration, particle diameter, and specimen configurations were tested sufficiently to determine the effect, if any, that they have on the results.

Effect of Angle of Attack

One of the more interesting features of erosion of ductile materials is the manner in which the angle at which particles strike the target surface influence the metal removal rate. Figure 5 illustrates these results for 2024 aluminum alloy at different particle velocities. For all of the velocities tested, the angle of maximum weight loss occurs at an angle of approximately 20°. As the angle of attack increases from this value, the erosion reduces to a residual value at 90°.

Effect of Particle Velocity

The early investigators of erosion proposed that the process was proportional to the kinetic energy of the oncoming particle. This predicted relationship (i.e., $\epsilon \sim V^2$) would almost intuitively be expected. However, the experimental observations have shown that the velocity exponent is normally greater than two. Finnie, et al.[11] found that a velocity ex-

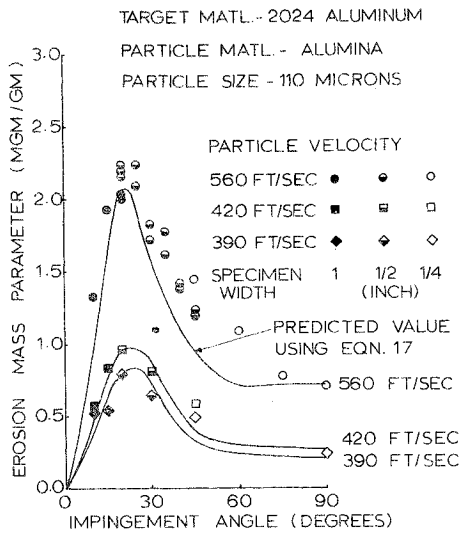

Fig. 5 Experimental and predicted erosion results.

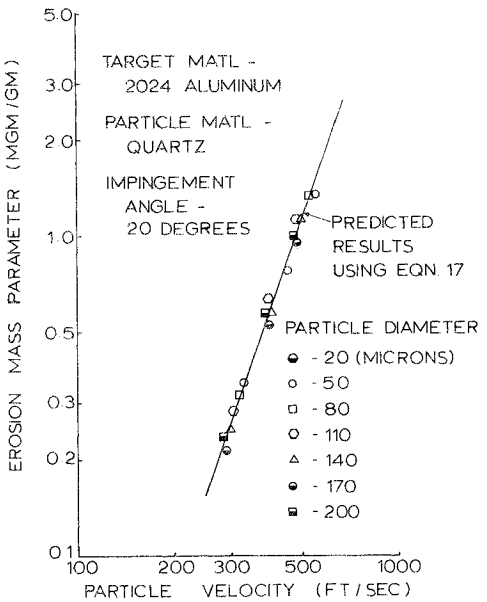

Fig. 6 Effect of velocity on erosion rate.

ponent as high as three could be expected if the cutting depth of the particle is assumed as a function of the material strength. Tilly and Sage[12] have proposed that the velocity exponent is greater than two as a result of particle fragmentation upon impact since the particle fragments flowing over the eroded surface cause secondary damage. Finally, Sheldon and Kanhere[13] developed a particle penetration equation based on indentation hardness theory which predicts that the velocity exponent may be as high as three. Despite these analyses, the exact reason for the velocity exponent being greater than two is perhaps the single most controversial issue in the study of erosion.

The effect of velocity was investigated at angles-of-attack 20° and 90°. These results are presented in Figs. 6 and 7. The influence at the other angles of attack was illustrated in Fig. 5. The data for 20° impact indicate that the velocity exponent is approximately 2.8 (i.e., $\epsilon \sim V^{2.8}$). At normal, or 90° impact, the velocity exponent is on the order of 4. To the knowledge of the author, this is the highest velocity exponent found in the literature. This may be due to the inclusion of the aerodynamic effects in the test facility. It was found that the particle size did not influence the erosion after a certain threshold value was reached. This threshold value is dependent upon both the particle velocity and particle size.

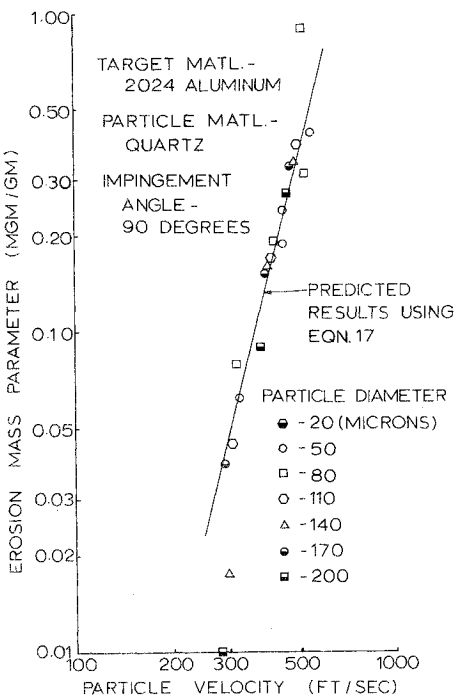

Fig. 7 Effect of velocity on erosion rate.

Prediction of Erosion on 2024 Aluminum Alloy

The measured erosion has been plotted against the primary parameters of angle-of-attack, particle velocity and particle size. These data were fit with the following equations.

$$\epsilon = K_1 f(\beta_1) V_1^2 \cos^2\beta_1 [1 - R_T^2] + f(V_{1N}) \quad (17)$$

$$R_T = 1 - 0.0016\, V_1 \sin\beta_1 \quad (18)$$

$$f(\beta_1) = [1 + CK(K_{12} \sin 2\beta_o)]^2 \quad (19)$$

$$f(V_{1N}) = K_3 (V_1 \sin\beta_1)^4 \quad (20)$$

The empirical constants for quartz impacting the aluminum alloy are: $K_1 = 3.67 \times 10^{-6}$; $K_{12} = 0.585$; and $K_3 = 6.0 \times 10^{-12}$. For a more detailed development of these equations, the reader is referred to Ref. 14.

Development of Model to Predict Erosion in Turbomachinery

Model Requirements

The basic information on particle dynamics and rebound characteristics has been developed such that the particle trajectories within turbomachinery can be predicted. The material removal process can then be predicted using this trajectory and impact data. However, for the complicated problem concerning the erosion of turbomachinery, this information alone is not sufficient. The equations developed thus far are homogeneous in nature, that is, they can be used to predict the erosion resulting from a given particle entering the machine at a given location and rebounding in a given manner. However, the physical problem of natural dust ingestion into turbomachinery is heterogeneous. The particles that are entrained in the inlet come in various sizes, shapes and composition. The location of the particle in the inlet can vary in the radial and circumferential directions. The initial location of the rotor relative to the stator is also a variable which will influence the results. Further, as was discussed previously, the particles do not always rebound in the same manner. Rather, the restitution ratios have been described in terms of a statistical distribution. The variation of all of these parameters will effect the location of impact as well as the quantity of material removed.

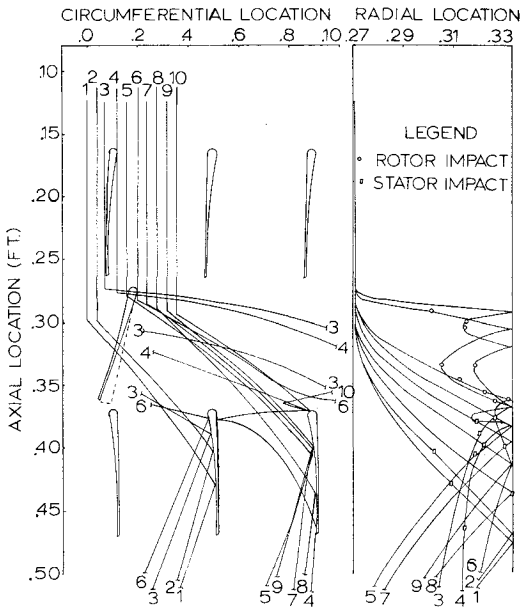

Fig. 8 Particle trajectories in a one and one-half stage compressor.

To account for these effects, a Monte Carlo simulation model of the process is developed. This model can simulate the dust ingestion and subsequent erosion in any single or multistage compressor or turbine provided that the design geometric variables are given. The input for the statistical distributions are particle size, particle location, rotor location, and restitution ratio. From these distributions, the specific conditions for the particle being investigated are chosen using a random number generator. By considering a statistically adequate number of particles (such as 10,000) the heterogeneous solution is obtained.

Predicted Particle Trajectories

The trajectories of 20 μ quartz particles, through a test model compressor were investigated. The one and one-half stage compressor consisted of inlet guide vanes followed by a compressor rotor and stator.

Fig. 8 illustrates the trajectories of ten particles uniformly entering at the hub of the inlet guide vane. Both the axial-circumferential and the axial-radial planes are plotted on this illustration, thus the three-dimensional nature of these trajectories is illustrated. The diameter of the flow channel is relatively small and as such the centrifugal effects on the particles are pronounced.

All of the particles initially impact the rotor near the leading edge. After this impact they rebound with a large tangential velocity component and rapidly centrifuge to the tip casing. Many of the particles rebound off the casing and strike the rotor blade again before reaching the discharge stator. The particles strike the stator on the outer one-third of the blade due to the centrifugal effects.

Erosion Patterns

The erosion profiles for a mixture of 2,400 g of quartz sand passing through a test compressor was evaluated using the analytical model. The erosion predicted to occur on the inlet guide vane is predominantly on the lower portion of the blade near the tip and on the side that would intercept the particles rebounding up off the leading edge of the rotor. The predicted erosion profile is given in Table 2. Almost all of the erosion predicted to occur on the rotor takes place near the leading edge. However, a quantity of erosion is also predicted to take place on the trailing edge of the rotor on the pressure surface. This damage results from particles rebounding up from the discharge stator. This explanation is substantiated by the fact that most of this damage occurs near the tip of the blade indicating considerable centrifuging. The erosion of the discharge stator is predicted to be approximately 37% less than that of the rotor. This is primarily because many of the particles impact the casing as the particle travels from the rotor to the discharge stator lowering the particle velocity. The erosion profile indicates that particles causing almost all the damage have previously rebounded off the rotor.

The one and one-half stage compressor was tested with quartz sand ingested at the inlet to obtain an experimental verification of the predicted results. The blades used in these tests were made of 2024 aluminum alloy and a rotor speed of

Table 2 Rotor Erosion (predicted[a])

	Radial location, ft (right suction side)						
Axial dist (ft)	0.2708 (hub)	0.2812	0.2916	0.3020	0.3125	0.3229	0.3333 (tip)
0.279	0.0	0.0001	0.0001	0.0000	0.0010	0.0014	0.0192
0.291	0.0	0.0	0.0	0.0	0.0	0.0006	0.0272
0.304	0.0	0.0	0.0	0.0	0.0	0.0004	0.1200
0.316	0.0	0.0	0.0	0.0	0.0	0.0032	0.0244
0.328	0.0	0.0	0.0	0.0	0.0	0.0006	0.0006
0.340	0.0	0.0	0.0	0.0	0.0	0.0004	0.0026
0.352	0.0	0.0001	0.0000	0.0002	0.0001	0.0003	0.0112
0.364	0.0	0.0	0.0	0.0	0.0	0.0010	0.0032
	Radial location, ft (left pressure side)						
Axial dist. (ft)	0.2708 (hub)	0.2812	0.2916	0.3020	0.3125	0.3229	0.3333 (tip)
0.279	1.5395	3.9289	4.0388	4.2171	4.8283	5.3429	3.0893
0.291	0.2324	0.5207	0.6335	0.6409	0.7196	0.8838	0.4989
0.304	0.0	0.0	0.0002	0.0004	0.0055	0.0180	0.0493
0.316	0.0	0.0	0.0	0.0013	0.0102	0.0328	0.0429
0.328	0.0	0.0	0.0	0.0	0.0111	0.0599	0.0754
0.340	0.0	0.0	0.0010	0.0000	0.0011	0.0492	0.1350
0.352	0.0	0.0	0.0	0.0611	0.0010	0.3452	0.2062

[a] The mass eroded from this blade is predicted to be 35.205 g. The quantity of quartz sand used is 2400 g.

12,400 rpm was obtained by overloading the motor. The maximum inlet length, 7 1/2 ft, was used so that the particle velocities were very close to the air velocities when they arrived at the test section.

The first series of tests conducted using this facility determined the location where majority of erosion took place on the blades. To accomplish this, the blades were painted black before the test. As the sand traveled through the test section, the paint wore off the region of the blade where the sand impacted. One problem with utilizing this experimental technique is that it does not provide a good comparison of the relative magnitude of the erosion. The paint wears off the regions of very high erosion almost immediately upon initiation of the test. As the test proceeds the paint also wears off the regions where a lesser amount of erosion takes place. These two regions then appear as having the same erosion wear. This factor was partially discounted by having a very short duration test.

The experimentally obtained erosion profiles, depicted in Fig. 9, compare favorably to the predicted profile. The erosion of the inlet guide vane takes place near the bottom of the blade. This pattern moves away from the hub and proceeds to the tip, when viewing the blade from the trailing edge. This is the same pattern that is predicted by the computer program. The primary cause of erosion on the inlet guide vane is a result of particles rebounding back from the rotor leading edge.

The rotor erosion profile, illustrated in Fig. 9, shows that the region at the center of the blade near the hub is eroded very little if at all. This coincides with the predicted profile included in Table 2. Practically all the particles impact the leading edge of the rotor, thus the magnitude of erosion there is understandable. Further, some particles rebound back from the leading edge of the discharge stator and cause erosion damage to the trailing edge of the rotor blades. Some of the sand particles will centrifuge to the tip casing after impacting the rotor. As these particles impact the casing they will lose a fraction of their velocity, allowing the rotor to again be impacted by them. This is most likely the primary cause of the erosion noted at the tip of the blade.

The region where the stator suffers greatest erosion, as depicted in Fig. 9, is the region adjacent to the leading tip of the blade. This profile results from the sand particles impacting the rotor and centrifuging toward the tip by the time they reach the stator. Since this profile again verifies the theoretical results the model has successfully predicted the regions where erosion takes place on all three blades. This quantitative agreement is very important, as it verifies that the predictive model properly accounts for the basic particle-blade-casing interaction.

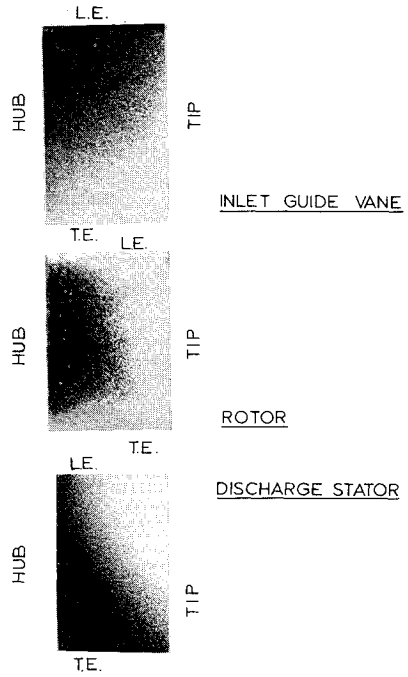

Fig. 9 Regions of blade erosions. Note: the light area indicates regions of erosions. L.E. = leading edge; T.E. = trailing edge.

Eroded Mass

To evaluate the ability of the model to predict quantitative results, a second set of tests were run. In these tests the detachable blades were weighed before and after a run in which a known amount of sand was injected into the inlet. In this manner, the magnitude of the erosion was measured. The results of these tests were given in Table 3.

The effect of particle size was the first parameter to be investigated in this series of tests. Three different tests were run using large particles (125-149 μ), small particles (44-77 μ), and a mixture of particle sizes. The predicted erosion of the rotor and discharge stator was within 20% of the measured values for all three tests. However, the erosion predicted for the inlet guide vane was only a fraction of that observed.

As a result of the disparity between the predicted and observed results the test section was torn down. The blades were found to be damaged to the extent that their geometric profiles were changed. The trailing edges of both the inlet guide vane and the rotor were shortened, and in some cases the blades were bent. The leading edge of the rotor blade had worn from its original circular profile to a flat surface.

The flat leading edge of the rotor was inclined at such an angle that a disproportionate number of particles were rebounding back to the stator, which resulted in the increase in erosion noted. For this reason, a new set of blades was installed into the facility. The first test on the old set of blades had been run with 4800g of sand. Two tests were run with the new set of blades using 2400g of sand for each test. In this manner the effect of the change of the leading edge geometry should be directly measured. The first test on this new set of blades resulted in a much reduced inlet guide vane erosion. In this case, the theoretical model predicted the erosion very accurately. After the test, it was observed that the leading edge of the rotor was beginning to wear. The subsequent test on this set of blades using another 2400g of sand, resulted in an inlet guide vane erosion almost three times as high as was the case of the first 2400g. The rotor leading edge was worn almost flat after this test. Thus, the results of these tests verify the hypothesis that the large difference between the predicted and observed erosion on the first set of experiments was due to the geometric change of the rotor leading edge.

Table 3 Comparison of experimentally observed and predicted erosion

Test no.	Rotor rpm	Sand mass mg	Particle size (Microns)	IGV erosion (mg)		Rotor erosion (mg)		Stator erosion (mg)	
				predicted	observed	pred.	obs.	pred.	obs.
1	12,400	4,800	(125-149)	4.4	29.0	72.0	83.2	46.0	27.2
2	12,400	1,175	(44-74)	0.72	5.2	18.3	23.4	9.3	11.9
3	12,400	1,300	(Mixture)	1.3	8.1	19.1	23.5	12.34	15.4
4	12,400	2,400	(Mixture)	2.3	2.9	35.2	39.3	22.8	21.2
5	12,400	2,400	(Mixture	2.3	7.9	35.2	32.4	22.8	25.9

Table 4 Effect of particle size on erosion in a one and one-half stage axial flow compressor

Particle Size (μ)	IGV (mg)	Rotor (mg)	Stator (mg)
20	0.13	40.8	8.4
50	1.03	37.4	17.6
80	1.40	36.4	21.1
120	2.20	36.1	22.7
140	2.70	35.8	22.7
170	2.94	35.9	23.3
200	3.38	35.6	23.3
Mixture	2.33	35.3	22.8

The data obtained from Test No. 4 are the only data obtained from blade geometries, the same as those inputed into the analytical model. As such, these data are used to verify the predicted results. The analytical model predicts the erosion of this test within 20% of the observed value on the inlet guide vanes, within 10% on the rotor, and within 7.5% on the discharge stator. For a more detailed description of the test results and their comparison to the predicted values, see Ref. 15.

Predicted Effects of Particle Size

Several runs were made to determine the influence of particle size on erosion. These results are listed on Table 4. In general, the influence of increasing particle size is such that the erosion of stationary blades increases and rotating blades decreases. The results can be traced to particle aerodynamic and erosion angle-of-attack considerations.

Conclusion

An analytical model has been developed to predict the erosion resulting from natural dust ingestion into turbomachinery. This model considered the aeroynamic drag on the dust particles, the rebound dynamics of the particle impacting the solid blades or channel walls, and the material removal process. The computerized model uses a Monte Carlo simulation of the process. This process involves the examination of a single particle, and the parameters concerning particle size, particle location, rotor location, and restitution ratio which are chosen from statistical distributions. By examining a statistically adequate number of particles the heterogeneous solution is determined.

The study shows that, in general, the erosion damage of an axial flow compressor is principally caused by the cutting back of the leading edge of the blade and the thinning of the trailing edge of the blade. The particles will centrifuge radially especially after impacting a rotor blade. The dust then becomes concentrated at the tip of the blades and cause severe damage at this location.

In addition, an experimental investigation was conducted to measure the erosion damage to a one and one-half stage compressor. These measured results are compared to the results predicted by the analytical model. The comparison is very favorable in that the analytical model not only predicts the magnitude of the erosion very closely, but it also gives the location on the blades where the erosion occurs.

References

[1] Goodwin, J. E., Sage, W., and Tilly, G. P., "Study of Erosion by Solid Particles," *Proceedings of the Institute of Mechanical Engineers*, Vol. 184, Pt. 1, 1969-70, pp. 279-292.

[2] Grant, G. and Tabakoff, W., "An Experimental Study of Certain Aerodynamic Effects on Erosion," Tech. Rept. 72-28, July 1973, University of Cincinnati, Cincinnati, Ohio.

[3] Grant, G. and Tabakoff, W., "A Quasi-Analytical Method for the Calculation of Particle Trajectories," Tech. Rept. 73-35, Feb. 1973, University of Cincinnati, Cincinnati, Ohio.

[4] Finnie, I. and Kabil, Y.H., "On the Formation of Surface Ripples During Erosion," *Wear*, Vol. 8, 1965, pp. 60-69.

[5] Finnie, I., "The Mechanism of Erosion of Ductile Metals," *ASME Proceedings of Applied Mechanics*, 1958, pp. 527-532.

[6] Smeltzer, C. W., Gulden, M. E., McElmury, S. S., and Compton, W. A., "Mechanism of Sand and Dust Erosion in Gas Turbine Engines," Technical Rept. 70-36, Aug. 1970, U.S Army Aviation Material Lab., Fort Eustis, Va.

[7] Grant, G., Ball, R., and Tabakoff, W., "An Experimental Study of the Erosion Rebound Characteristics of High Speed Particles Impacting a Stationary Specimen," Tech. Rept. 73-36, University of Cincinnati, Cincinnati, Ohio, AD-760578, May 1973.

[8] Hussein, M. F., "The Dynamic Characteristics of Solid Particulated Flow in Rotating Machinery," Ph.D. thesis,Dept. of Aerospace Engineering, 1972, University of Cincinnati, Cincinnati, Ohio.

[9] Head, W. J., "The Development of a Model to Predict the Erosion of Materials by Natural Contaminants," Ph.D. thesis, Dept. of Civil Engineering, 1970, Purdue University, West Lafayette, Ind.

[10] Tabor, D., *The Hardness of Metals*, 1st ed., Clarendon Press, Oxford, England, 1951.

[11] Finnie, I., Wolak, J., and Kabil, Y., "Erosion of Metals by Solid Particles," *Journal of Materials*, Vol. 2, Sept. 1967, pp. 682-700.

[12] Tilly, G. P. and Sage, W., "The Interaction of Particle and Material Behaviro in Erosion Processes," *Wear*, Vol. 16, 1970, pp. 447-465.

[13] Sheldon, G. L. and Kanhere, A., "An Investigation of Impingement Erosion Using Single Particles," *Wear*, Vol. 21, 1972, pp. 195-209.

[14] Grant, G. and Tabakoff, W., "An Experimental Investigation of the Erosive Characteristics of 2024 Aluminum Alloy," AD-764267, Tech. Rept. 73-37, June 1973, University of Cincinnati, Cincinnati, Ohio.

[15] Grant, G., "A Model to Predict Erosion in Turbomachinery Due to Solid Particles in Particulated Flow," Ph.D. thesis, Dept. of Aerospace Engineering, 1973, University of Cincinnati, Cincinnati, Ohio.